Acta Crystallographica Section D
Biological Crystallography
ISSN 0907-4449

RARβ ligand-binding domain bound to an SRC-1 co-activator peptide: purification, crystallization and preliminary X-ray diffraction analysis

Sabrina Kammerer,[a] Pierre Germain,[b] Ralf Flaig,[a] Carole Peluso-Iltis,[a] André Mitschler,[a] Natacha Rochel,[a] Hinrich Gronemeyer[b] and Dino Moras[a]*‡

[a]Department of Structural Biology and Genomics, Institut de Génétique et de Biologie Moléculaire et Cellulaire, France, and [b]Department of Cell Biology and Signal Transduction, Institut de Génétique et de Biologie Moléculaire et Cellulaire, France

‡ Current address: IGBMC, BP 10142, 1 Rue Laurent Fries, 67404 Illkirch CEDEX, France.

Correspondence e-mail: moras@igbmc.u-strasbg.fr

Received 26 July 2004
Accepted 30 August 2004

Retinoids have demonstrated therapeutic efficacy in the treatment of acute promyelocytic leukaemia and in the chemoprevention of a large number of cancers. As the cellular signalling pathway of retinoids can be transduced by the three retinoic acid receptor (RAR) isotypes α, β and γ, the side effects of these treatments induced efforts to generate isotype-selective ligands. Despite knowledge of the crystal structures of RARα and RARγ ligand-binding domains (LBDs), the rational design of such ligands has been hampered by the absence of RARβ LBD structural data. Here, a strategy used to express a large-scale soluble fraction of the human RARβ LBD suitable for biophysical analysis is reported, as well as a procedure for crystallizing it bound to a synthetic retinoid (TTNPB) with or without a co-activator peptide (SRC-1). Preliminary X-ray analysis revealed that both complexes crystallized in the orthorhombic space group $P2_12_12_1$. The unit-cell parameters are a = 47.81, b = 58.52, c = 92.83 Å for the TTNPB–hRARβ LBD crystal and a = 58.14, b = 84.07, c = 102.37 Å when the SRC-1 peptide is also bound.

1. Introduction

Retinoids (vitamin A derivatives) are crucial to prenatal and postnatal development and during adult life as they regulate important cellular events such as differentiation, proliferation and apoptosis (Chambon, 1996). Retinoic acid receptor (RAR) α, β and γ isotypes, which have distinct but partially redundant functions (Kastner *et al.*, 1995), transduce the pleiotropic effects of retinoids in the cell and are thus therapeutic targets for cancer therapy. Retinoids are indeed currently used for the treatment of acute promyelocytic leukaemia and for the chemoprevention of many types of cancer (Altucci & Gronemeyer, 2001).

RARs belong to the superfamily of nuclear receptors (NRs), which are ligand-inducible transcription factors activating the transcription by co-activator recruitment. NRs display a modular structure with differentially conserved regions (named regions A–F; Laudet & Gronemeyer, 2002), regions C and E being the most highly conserved. Region C encompasses the DNA-binding domain (DBD) and region E the ligand-binding domain (LBD) as well as a ligand-dependent transactivation function (referred to as AF-2). X-ray structures of several liganded (holo) and unliganded (apo) receptors showed that NR LBDs share an evolutionarily conserved fold composed of 12 α-helices and an antiparallel β-sheet. They subsequently share a common ligand-binding and receptor-activation mechanism: the ligand-induced repositioning of helix H12 in the holo-LBD provides the surface for co-activator interaction and thereby generates the transcriptional activity of the AF-2 domain (Bourguet, Germain *et al.*, 2000).

Observation of the side effects of retinoid therapy as well as the specific actions of RAR isotypes have induced efforts to generate isotype-selective retinoids. X-ray analysis of agonist-bound RARγ (Renaud *et al.*, 1995) and antagonist-bound RARα (Bourguet, Vivat *et al.*, 2000) LBDs have revealed insight into the structural basis of the RAR-isotype selectivity (Klaholz *et al.*, 1998; Klaholz, Mitschler, Belema *et al.*, 2000; Klaholz, Mitschler & Moras, 2000). Nevertheless, the RARβ LBD structure could not be solved to date owing to the poor expression level and solubility of this protein (Love *et al.*, 2002). However, RARβ is of a particular interest as it has been speculated to act as a tumour suppressor (Widschwendter *et al.*, 2001; Sun & Lotan, 2002; Sirchia *et al.*, 2002). Moreover, it interacts only very poorly with co-repressor; thus, it is possible that its tumour-inhibitory effect could be partially correlated with this RARβ function.

The structural study of hRARβ LBD bound to the RAR panagonist TTNPB with or without the coactivator SRC-1-derived peptide (SRC-1 peptide) has been carried out in order to provide detailed information on the RARβ ligand-binding site (1.9–2.1 Å) as well as to

characterize the influence of the peptide binding on the RAR LBD conformation and particularly on the repositioning of helix H12.

In this paper, we report the strategy used to express a large-scale soluble fraction of the hRARβ LBD suitable for biophysical analysis and the crystallization conditions of the TTNPB–hRARβ LBD complex with or without the SRC-1 peptide. We also present the preliminary X-ray analysis of these complexes.

2. Experimental procedures and results

2.1. Protein expression and purification

The human RARβ LBD (residues 173–409) was cloned as a His-tag fusion protein into the pET15b vector and expressed in *Escherichia coli* cells. The transformed cells were plated onto LB agar containing 200 µg ml^{-1} ampicillin. Overnight precultures of hRARβ LBD-pET15b-transformed BL21(DE3) were used to start large-scale protein production. Cultures were grown at 310 K in LB medium containing 200 µg ml^{-1} ampicillin and 5% sucrose to an OD_{600} of 0.4 and expression of the T7 RNA polymerase was induced by adding 0.5 m*M* IPTG (Studier *et al.*, 1990). The culture medium was then cooled to 288 K. After an additional incubation of 3 h, 6 l of hRARβ LBD culture was pelleted and resuspended in 75 ml cold buffer *A* (5 m*M* imidazole, 500 m*M* NaCl, 20 m*M* Tris pH 8.0). Lysis was performed by adding 100 µg ml^{-1} lysozyme followed by 30 min on ice and 5 min at 310 K and finally by 3 × 2 min sonication. 75 ml cold buffer *A* was added after the first 2 min sonication. All subsequent steps were performed at 277 K. The hRARβ LBD soluble fraction was isolated by 20 000 rev min^{-1} centrifugation for 45 min.

The supernatant was loaded onto an Ni HiTrap chelating column (Amersham Biosciences) equilibrated with buffer *A*. After two wash steps with 30 volumes of buffer *A* and buffer containing 50 m*M* imidazole, the protein was eluted with buffer *A* containing 150 m*M* imidazole. A Bradford assay as well as SDS–PAGE and silver-staining analysis were used to further characterize the fractions. The hRARβ LBD-containing fractions were pooled and diluted twice in buffer *B* (300 m*M* NaCl, 5 m*M* DTT, 10 m*M* Tris pH 7.5). The protein was then concentrated to a volume of 5 ml and loaded onto a Superdex 75 16/60 gel-filtration column (Amersham Biosciences) pre-equilibrated with buffer *B*. The fractions containing hRARβ were pooled after SDS–PAGE characterization and a twofold molar excess of ligand as well as a threefold molar excess of SRC-1 coactivator peptide (CPSSHSSLTERHKILHRLLQEGSPS, containing the L*xx*LL motif mediating coactivator binding) for the ternary complex were added. After overnight incubation, the complexes were concentrated for crystallization. The complexes were estimated to be more than 95% pure as judged from the silver-stained gel (Fig. 1).

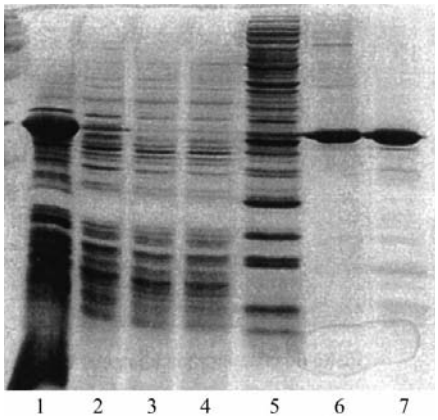

Figure 1
Purification of hRARβ LBD. A 12% SDS–PAGE gel of the purification pools was silver-stained. Lane 1, pellet; lane 2, soluble crude extract; lane 3, flow-through; lane 4, first wash (5 m*M* imidazole); lane 5, second wash (50 m*M* imidazole); lane 6, Ni pool; lane 7, gel-filtration pool.

2.2. Crystallization of the TTNPB–hRARβ and TTNPB–SRC-1–hRARβ LBD complexes

The crystallization screening was carried out by the sitting-drop vapour-diffusion method using Hampton Research crystallization screens and 96-well Greiner plates. Typically, 3 µl sitting drops were obtained by mixing equal volumes of the concentrated protein solution and the reservoir solution; the wells contained 150 µl reservoir solution. A diffraction-quality crystal of the TTNPB–hRARβ LBD complex grew in 9 d at 290 K from crystallization condition No. 5 of the Natrix screen (Hampton Research) containing 5% polyethylene glycol 8000, 0.2 *M* KCl, 0.01 *M* $MgCl_2$ and 0.05 *M* MES pH 5.6. Its final dimensions were 0.3 × 0.07 × 0.05 mm. TTNPB–SRC-1–hRARβ LBD crystals were also grown at 290 K in 8 d from 25% polyethylene glycol 4000, 0.1 *M* trisodium citrate dihydrate pH 5.5 to final dimensions of 0.25 × 0.07 × 0.04 mm (Fig. 2).

2.3. X-ray data collection and data processing

TTNPB–hRARβ LBD crystals were mounted in a cryoloop (Hampton Research) and flash-cooled in liquid ethane at liquid-nitrogen temperature in 5% polyethylene glycol 8000, 0.2 *M* KCl, 0.01 *M* $MgCl_2$, 0.05 *M* MES pH 5.6 with 25% glycerol. X-ray diffraction data were collected at λ = 0.8856 Å using a MAR CCD detector (165 mm) at beamline X06SA of the Swiss Light Source (SLS, Villigen, Switzerland) with an oscillation range of 0.5° per frame at 100 K. The crystals of TTNPB–hRARβ LBD bound to the SRC-1 peptide were flash-cooled at liquid-nitrogen temperature in a cryoprotection solution consisting of the crystallization solution with 25% ethylene glycol. The data were collected at λ = 1.0093 Å at beamline ID14EH4 of the European Synchrotron Radiation Facility (ESRF, Grenoble, France) using a Quantum ADSC Q4R detector with an oscillation range of 0.5° at 100 K.

The data were processed using *DENZO* and scaled and merged with *SCALEPACK* (Otwinowski & Minor, 1997). The TTNPB–hRARβ LBD crystal diffracted to better than 2.1 Å resolution. The space group was $P2_12_12_1$ and the unit-cell parameters were $a = 47.81, b = 58.52, c = 92.83$ Å, $\alpha = \beta = \gamma = 90°$. The crystal of the TTNPB–hRARβ LBD complexed with the SRC-1 peptide diffracted to 1.9 Å resolution. The complex also crystallized in space group $P2_12_12_1$ but with unit-cell parameters $a = 58.14, b = 84.07, c = 102.37$ Å, $\alpha = \beta = \gamma = 90°$. Data-collection statistics are given in Table 1.

For the TTNPB–hRARβ LBD complex the data set between 20 and 2.1 Å was 98.7% complete (14 703 unique reflections) with an overall R_{sym} of 5.2%. In the last resolution

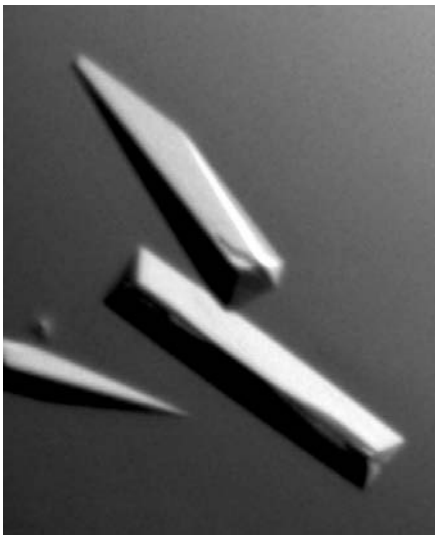

Figure 2
Crystals of the TTNPB–SRC-1–hRARβ LBD complex. The crystals were obtained in 25% polyethylene glycol 4000, 0.1 *M* trisodium citrate dihydrate pH 5.5. The largest crystals are of approximate dimensions 0.25 × 0.07 × 0.04 mm.

Table 1
Data-collection statistics.

Values in parentheses refer to the highest resolution shell (2.17–2.1 Å for TTNPB–RARβ LBD and 1.97–1.9 Å for TTNPB–RARβ LBD–SRC-1 peptide).

	TTNPB–hRARβ LBD	TTNPB–hRARβ LBD–SRC-1 peptide
X-ray source	SLS beamline X06SA	ESRF beamline ID14-4
Oscillation range (°)	0.5	0.5
No. frames	300	300
Space group	$P2_12_12_1$	$P2_12_12_1$
Unit-cell parameters (Å, °)	a = 47.81, b = 58.52, c = 92.83, $\alpha = \beta = \gamma = 90$	a = 58.14, b = 84.07, c = 102.37, $\alpha = \beta = \gamma = 90$
Z	1	2
Resolution limit (Å)	2.1	1.9
Total reflections	57705	197687
Unique reflections	14703	39762
Completeness (%)	98.7 (98)	98.4 (100.0)
Multiplicity	3.9	5.0
R_{sym} (%)	5.2 (27.1)	7.0 (40.6)
$I/\sigma(I)$	24.3 (3.5)	27.2 (5.3)
Matthews coefficient (Å^3 Da^{-1})	2.029	1.955
Solvent content (%)	37.05	34.65

shell (2.17–2.1 Å) R_{sym} was 27.1%, with a completeness of 98% [$I/\sigma(I)$ = 4.9]. Initial phases were obtained by molecular replacement using *CNS* (Brünger *et al.*, 1998) with the 9-*cis* RA–hRARγ LBD structure as search model (Klaholz *et al.*, 1998; PDB code 3lbd). All water and ligand molecules were removed from the model. The correct solution for the TTNPB–hRARβ LBD complex corresponding to one monomer in the asymmetric unit had a correlation coefficient CC = 58% and an R factor of 43.1% (the values for the next highest solution are CC = 18% and R = 56.0%). The crystal packing was checked and showed no clashes. In addition, interpretable electron density confirmed the molecular-replacement solution. The quality of the map allowed the clear identification of electron density for the TTNPB molecule at the beginning of the structure refinement and characterization of the expected agonist conformation of helix H12.

For the TTNPB–hRARβ–SRC-1 peptide complex the data set between 20 and 1.9 Å was 98.4% complete (39 762 unique reflections) with an overall R_{sym} of 7.0%. One dimer was observed in the asymmetric unit. The top molecular-replacement solution provided by *AMoRe* (Navaza, 1994) was CC = 39.5%, R factor = 41.6% (next highest solution: CC = 17.7% and R = 48.1%). According to the electron density, helix H12 appeared to be in the expected agonist conformation and the electron density of the TTNPB and the SRC-1 peptide became apparent at the beginning of the structure refinement. The refinement of this structure is in progress.

3. Concluding remarks

Both refined structures will be published elsewhere and should allow insight into RAR-isotype selectivity by showing the RARβ ligand-binding site for the first time. The availability of selective ligands for each of the three RAR isotypes will help to assess the role of the suspected tumour suppressor RARβ and aid in the generation of novel retinoids with reduced side effects, as retinoids are well established cancer-therapeutic and cancer-preventive agents. Moreover, a comparative study of the agonist-bound hRARβ LBD complex with and without the coactivator peptide should help to precisely define the influence of the coactivator binding on the RAR LBD conformation.

We thank Thierry Lerouge for plasmids and Pascal Eberling for peptide synthesis, William Bourguet for helpful discussions and the beamline staff at Swiss Light Source (SLS, Villigen, Switzerland) and at the European Synchrotron Radiation Facility (ESRF, Grenoble, France) for technical assistance during data collection. SK received fellowships from the MRT and the ARC; PG was supported by EU grants. This work was supported by the Fondation de France, the AICR, the ARC, the ULP, the INSERM and the CNRS.

References

Altucci, L. & Gronemeyer, H. (2001). *Nature Rev. Cancer*, **1**, 181–193.
Bourguet, W., Germain, P. & Gronemeyer, H. (2000). *Trends Pharmacol. Sci.* **21**, 381–388.
Bourguet, W., Vivat, V., Wurtz, J. M., Chambon, P., Gronemeyer, H. & Moras, D. (2000). *Mol. Cell*, **5**, 289–298.
Brünger, A. T., Adams, P. D., Clore, G. M., DeLano, W. L., Gros, P., Grosse-Kunstleve, R. W., Jiang, J.-S., Kuszewski, J., Nilges, M., Pannu, N. S., Read, R. J., Rice, L. M., Simonson, T. & Warren, G. L. (1998). *Acta Cryst.* D**54**, 905–921.
Chambon, P. (1996). *FASEB J.* **10**, 940–954.
Kastner, P., Mark, M. & Chambon, P. (1995). *Cell*, **83**, 859–869.
Klaholz, B. P., Mitschler, A., Belema, M., Zusi, C. & Moras, D. (2000). *Proc. Natl Acad. Sci. USA*, **97**, 6322–6327.
Klaholz, B. P., Mitschler, A. & Moras, D. (2000). *J. Mol. Biol.* **302**, 155–170.
Klaholz, B. P., Renaud, J. P., Mitschler, A., Zusi, C., Chambon, P., Gronemeyer, H. & Moras, D. (1998). *Nature Struct. Biol.* **5**, 199–202.
Laudet, V. & Gronemeyer, H. (2002). *The Nuclear Receptor Facts Book*. San Diego: Academic Press.
Love, J. D., Gooch, J. T., Benko, S., Li, C., Nagy, L., Chatterjee, V. K., Evans, R. M. & Schwabe, J. W. (2002). *J. Biol. Chem.* **277**, 11385–11391.
Navaza, J. (1994). *Acta Cryst.* A**50**, 157–163.
Otwinowski, Z. & Minor, W. (1997). *Methods Enzymol.* **276**, 307–326.
Renaud, J. P., Rochel, N., Ruff, M., Vivat, V., Chambon, P., Gronemeyer, H. & Moras, D. (1995). *Nature (London)*, **378**, 681–689.
Sirchia, S. M., Ren, M., Pili, R., Sironi, E., Somenzi, G., Ghidoni, R., Toma, S., Nicolo, G. & Sacchi, N. (2002). *Cancer Res.* **62**, 2455–2461.
Studier, F. W., Rosenberg, A. H., Dunn, J. J. & Dubendorff, J. W. (1990). *Methods Enzymol.* **185**, 60–89.
Sun, S. Y. & Lotan, R. (2002). *Crit. Rev. Oncol. Hematol.* **41**, 41–55.
Widschwendter, M., Berger, J., Muller, H. M., Zeimet, A. G. & Marth, C. (2001). *J. Mammary Gland Biol. Neoplasia*, **6**, 193–201.